DEUTSCHES ELEKTRONEN-SYNCHROTRON DESY

DESY SR 88-06
November 1988

Cluster–MO–Calculations on Germanium adsorbed on Si(111) Surfaces

M. Grodzicki, M. Wagner
Hamburger Synchrotronstrahlungslabor HASYLAB at DESY, Hamburg

Eigentum der DESY Bibliothek
Property of DESY library
Zugang: Accessions: 03. JAN. 1989
Leihfrist: Loan period: 7 Tage days

ISSN 0723-7979

NOTKESTRASSE 85 · 2 HAMBURG 52

DESY behält sich alle Rechte für den Fall der Schutzrechtserteilung und für die wirtschaftliche Verwertung der in diesem Bericht enthaltenen Informationen vor.

DESY reserves all rights for commercial use of information included in this report, especially in case of filing application for or grant of patents.

To be sure that your preprints are promptly included in the
HIGH ENERGY PHYSICS INDEX ,
send them to the following address (if possible by air mail) :

DESY
Bibliothek
Notkestrasse 85
2 Hamburg 52
Germany

DESY SR 88-06
November 1988

ISSN 0723-7979

Cluster-MO-Calculations on Germanium
adsorbed on Si(111) Surfaces

Michael Grodzicki and Marcus Wagner
Hamburger Synchrotonstrahlungslabor HASYLAB at DESY,
Notkestrasse 85, D-2000 Hamburg 52, Germany

Abstract

Cluster model calculations on Germanium adsorption onto the Si(111)-7x7 surface are performed with the SCC-Xα method. Calculations on small Si-clusters and on the bare substrate prove the model's reliability for the subsequent investigations comprising adsorption of a single Ge atom on two different sites in the DAS-model, as well as that of two Ge atoms simultaneously. Adsorption energies, distances and strengths of the respective Si-Ge-bonds are compared. Eventually, an explanation for the first steps of an interface formation between Si and Ge is offered.

to be published in Phys. Rev. B

Eigentum der DESY Bibliothek
Property of DESY library
Zugang: 03. JAN. 1989
Accessions:
Leihfrist: 7 Tage
Loan period: days

1 Introduction

The structure of the Si(111) surface including adsorption processes is a subject of central interest. Nevertheless, sufficient theoretical information is still missing from literature to interpret experimental data unambiguously and to investigate physical properties not amenable to experimental observation. In this article, we present the first calculation of Ge adsorption on a Si(111)-7x7 surface to provide some insight into the initial steps of Ge layer growth on silicon reconstructed in the DAS-Model of Takayanagi *et al*[1,2].

The interaction between a silicon substrate and germanium adsorbates is treated in the frame of the cluster model constituting an efficient procedure to handle such computations. The analysis is performed with the SCC-Xα method[3] which is a semiempirical procedure for calculating the electronic structure of large quantum mechanical systems. This method has already been successfully applied to problems such as the adsorption of water dimers on nickel[4,5], the adsorption of various molecules in zeolites[6,7,8] and the reaction of CO with an imperfect TiO_2 surface[9,10]. In section 2, calculations on small silicon clusters are reported for the comparison of the SCC-Xα method with ab initio investigations. In section 3, we discuss the results of our cluster calculations on the bare Si(111)-7x7 surface followed by the treatment of the Ge adsorption on this substrate in section 4 and a comparison of the results with the experiment in section 5. We conclude with a brief summary and an outlook on future perspectives and projects.

2 Calculations on Small Silicon Clusters

In this section we discuss briefly our calculations on the clusters Si_4 and Si_5 in some geometries resembling the silicon bulk coordination. This permits a comparison of the SCC-Xα method[3] with other procedures as well as an estimate of the reliability of our results when applied to modelling the Si(111)-7x7 surface. It should be pointed out that no experimental information on the silicon clusters dealt with in this work has yet been published. Our numerical results are summarized in table I.

The cluster Si_4 is computed for the two geometries corresponding to symmetries D_{4h} (square) and T_d (tetrahedron), respectively. For $Si_4(D_{4h})$ we obtain the same valence electron configuration $^3A_{2g}$: $(1a_{1g})^2$ $(1e_u)^4$ $(1b_{1g})^2$ $(1b_{2g})^2$ $(1a_{2u})^2$ $(2a_{1g})^2$ $(2e_u)^2$ as Raghavachari[11] from ab initio Hartree-Fock calculations and as Pacchioni and Koutecky (PK)[12] from an ab initio procedure including some configuration interaction, the latter authors obtaining only an interchange of the 2nd and 3rd highest levels. For T_d-symmetry our configuration $^1A_1$: $(1a_1)^2$ $(1t_2)^6$ $(2a_1)^2$ $(2t_2)^6$ is again identical with that of Raghavachari[11] while PK[12] compute, as the ground state, a triplet configuration being, however, only lower in energy by 0.003 eV than the $^1A_1$ configuration. Our bond lengths for Si_4 in D_{4h}- and T_d-symmetry of 2.198 A and 2.342 A, respectively, are slightly shorter than those of Raghavachari[11] with 2.316 A and 2.458 A. The bond lengths computed by PK[12] seem to be unreasonably large with 2.47 A and 2.71 A, respectively. Comparing the two symmetries with each other we obtain the D_{4h} distinctly more stable in qualitative agreement with Raghavachari[11] and PK[12] but in contrast to an older Hückel calculation of Martin and Schaber[13]. Our result is supported by the fact that the overlap population between two adjacent Si atoms in D_{4h} geometry of 0.886 e indicates a considerably stronger covalent bond than in T_d geometry with 0.453 e. This is easily understood because the bonds in the tetrahedron can be characterized as banana bonds being energetically less favourable than the unstrained ($pp\sigma$) bonds in the D_{4h} geometry.

Si_5 (cf. Fig. 1) is computed for three geometries corresponding to the symmetries D_{3h} (trigonal bipyramid), C_{4v} (square pyramid) and T_d (tetrahedron). According to our results, the trigonal bipyramid has the closed shell valence electron configuration $^1A_1'$: $(1a_2')^2$ $(1a_2'')^2$ $(1e')^4$ $(2a_1')^2$ $(1e'')^4$ $(3a_1')^2$ $(2e')^4$ with a lateral Si-Si distance of 2.991 A and a bond length between lateral and axial atoms of 2.342 A. The respective bond lengths of Raghavachari[11] are 3.256 A and 2.338 A. The bound state is only constituted by the lateral-axial bonds whereas the small negative overlap populations between two lateral atoms (-0.02 e) and between the two axial atoms (-0.06 e) exhibit a weak repulsion. The calculation of PK[12] has to be considered as unreliable in so far that they assume equal next neighbour distances of 2.63 A for the lateral-lateral and the lateral-axial bonds. This is most likely the reason why their calculated ground state is a triplet configuration.

In C_{4v}-symmetry we get a lateral bond length of 2.306 A, a lateral-axial bond length of 2.491 A and the configuration $^1A_1$: $(1a_1)^2$ $(1e)^4$ $(2a_1)^2$ $(1b_2)^2$ $(1b_1)^2$ $(3a_1)^2$ $(2e)^4$ $(4a_1)^2$ in almost perfect agreement with Raghavachari[11] whose atomic distances are 2.295 A and 2.502 A, respectively. Once more, the results of PK[12] have to be discarded because of their assumption of equal bond lengths. The overlap population of 0.695 e between two lateral atoms vs. 0.329 e between the axial atom and one lateral atom indicates much stronger covalent bonding within the square. The axial atom is negatively charged by -0.08 e leading to positive charges of 0.02 e at the lateral sites.

In tetraedral geometry we compute an $^1A_1$: $(1a_1)^2$ $(1t_2)^6$ $(2a_1)^2$ $(2t_2)^6$ $(1e)^4$ valence electron configuration with a bond length of 2.171 A. The calculation of PK[12] yields 2.50 A in a ^5E ground state configuration, both results appearing rather unlikely. In agreement with PK[12] we derive from the overlap population of 0.82 e between the central atom and a peripheral atom that these interactions constitute the stability of tetrahedral Si_5, the overlap charge between two peripheral atoms being only 0.01 e. The effective charges of 0.128 e for the central atom and -0.032 for each peripheral atom due to internal charge fluctuations should slightly stabilize this cluster and

shorten the bond length. The smooth potential curve of $Si_5(T_d)$ shows an extremely weak bonding and Raghavachari and Logovinsky[14] suppose this cluster even to be unstable. This conclusion, however, could be due to the neglect of the Coulomb correlations in Hartree-Fock becoming especially important when strong repulsive non-bonding interactions between lone pair orbitals occur, as it is also the case in F_2.

We obtain Si_5 to be most stable in D_{3h}-symmetry which agrees with Raghavachari[11] but not with PK[12] who favour a planar C_{2v}-geometry, maybe due to unreasonable geometry restrictions in the case of D_{3h} and C_{4v}. Therefore, D_{3h} is proposed to be the ground state geometry for Si_5.

Altogether, the SCC-Xα bond lengths agree with the Hartree-Fock results of Raghavachari[11] within 5 % or better which proves that Si-Si bonds are well described in the frame of the SCC-Xα method and that reliable results can be expected also for calculations on the silicon surface.

3 The clean Si(111) Surface

The solid state model and the cluster model are two approaches to treat adsorption phenomena on solid surfaces, which mainly differ in modelling the substrate. The solid state model assumes it as a two-dimensional ideal surface only weakly disturbed by the adsorbate. For several reasons, viz. problems with self-consistency, non-ideal substrate surfaces and determination of adsorption geometries via total energy calculations, the solid state model is not a suitable approach in our case. Within the cluster model the adsorption site and its environment are represented by a finite cluster; this approach is applicable if the adsorption can be assumed to be in good approximation a local phenomenon[15]. Although the cluster model is less realistic it offers several practical advantages compared to the solid state model concerning the treatment of non-ideal surfaces and the determination of adsorption geometries, in particular. The well known drawbacks of the cluster model, viz. the size problem, internal charge fluctuations, and the embedding problem can be treated by meanwhile standard techniques, described e.g. in Hütsch[9].

The only theoretical work on a Si(111)-7x7 surface reconstructed in the DAS-Model is a recent calculation of Qian and Chadi[17] which is, however, non-selfconsistent and restricted to next neighbour interactions. Even though the simplicity of this approach allows the handling of a cluster of 200 Si atoms and 49 H atoms, and determining of its equilibrium geometry, it precludes, e.g., the distinction between an fcc and an hcp lattice since for tetrahedral coordinated atoms the next neighbour environments are equal in both cases. Thus the stacking fault in the DAS-Model cannot be accounted for but has to be introduced as an assumption.

In the SCC-Xα Method[3] the interatomic potential matrix elements are not parametrized but explicitly calculated through

$$V_{ij}^{\mu\nu} = \int d^3r\, \varphi_i^{(\mu)}(\vec{r}-\vec{R}_\mu)\Big[\sum_{\mu\neq\nu} V_{at}^{(\kappa)}(\vec{r}-\vec{R}_\kappa)\Big]\varphi_j^{(\nu)}(\vec{r}-\vec{R}_\nu) \tag{1}$$

where $\varphi_i^{(\mu)}(\vec{r}-\vec{R}_\mu)$ denotes the $(n_i l_i m_i)$ real atomic valence orbital of the atom μ located at R_μ. The atomic potential $V_{at}^{(x)}$ is described in the $X\alpha$-approximation, and the sum includes all cluster atoms x removing the restriction to next neighbour interactions. Moreover, the resulting secular equation is solved selfconsistently with respect to atomic orbital occupation numbers

$$x_i^\mu = 2a_i^\mu \sum_{\nu j} S_{ij}^{\mu\nu} P_{ij}^{\mu\nu} / (a_i^\mu + a_j^\nu) \tag{2}$$

which are constructed from the overlap matrix $S_{ij}^{\mu\nu}$ and the bond-order matrix elements

$$P_{ij}^{\mu\nu} = \sum_k n_k c_{ik}^\mu c_{jk}^\nu \tag{3}$$

where n_k are the occupation numbers of the molecular orbitals (MOs) and the weight factors[18] are introduced in order to overcome the drawbacks of the Mulliken population analysis in a simple way. Whereas the SCC-$X\alpha$ calculations should yield more reliable results, it imposes limitations upon the cluster size for handling the system within reasonable computation time. In our case, the minimal cluster size is determined by the requirement of including at least the next nearest neighbours of each adsorption site because it has turned out that these are still affected by Ge adsorption. Consequently, we selected a $Si_{28}H_{26}$ cluster (cf. Fig. 2) to model the Si(111)-7x7 surface as the substrate for Ge adsorption. As usual, the H-atoms serve to saturate the Si-bonds on the artificial surface arising from cutting the cluster out of the bulk. The average effective charge of all Si bulk atoms including those of the artificial surface amounts to 0.031 ± 0.031 e so that the internal charge fluctuations are sufficiently suppressed. The computation time for this 138 valence orbital cluster amounts to 95 sec per iteration on a Siemens 7.882 computer being approximately 8-10 times slower than a Cray 1.

Starting from the equilibrium geometry as calculated by Qian and Chadi[17] we have checked the equilibrium positions of those Si-atoms where Ge adsorption takes place, namely the surface site (atom 6, cf. Fig. 2a) and the adatom (atom 1). Defining the surface as the average z-coordinate of those surface atoms (no. 2, 3, 4, 5, 7, 8, 9, cf. Fig. 2a) saturated by an adatom in the DAS-Model, the height of the adatom is 1.266 A corresponding to an average bond distance of 2.461 A to the neighbouring atoms 3, 5, 7 in almost perfect agreement with the results of Qian and Chadi[17], our bond lengths being only 0.028 A shorter. On the other hand, the height of the surface site over the surface is 0.068 A giving an average bond length to its next neighbour atoms 13, 15, 17 of 2.310 A which is shorter by 0.100 A than the respective value of Qian and Chadi[17]. This does not seem to be a large deviation but the corresponding heights of atom 6 over the surface differ significantly, Chadi and Qian's[17] surface site protruding by 0.261 A over the surface. However, it should be noticed that our calculated distance is slightly closer to the Si bulk bond length of 2.35 A.

The reason for the differences for these two sites could originate from higher order neighbour interactions. For, the surface atom is in a real "hollow site" with an atom underneath only in the 6th layer, whereas the adatom resides essentially in a "top site" because the atom 14 (hidden from view in Fig. 2 by the adatom) is located directly below at a distance of 2.441 A. For decreasing distances the adatom will be prevented from sinking into the bulk by atom 14 while such an argument does not apply to the surface site. This effect, however, can be only taken into account if there is no restriction to interaction between sp^3 bonded partners. Northrup[19] and Qian and Chadi[17] calculate the distance between the adatom and the atom 14 to be 2.49 A which is 2 % above our value of 2.44 A while Daum, Ibach, Müller[20] obtain 2.32 A which is 5 % below. From the short separation one cannot, however, conclude that the adatom is fivefold coordinated, as do Daum, Ibach and Müller[20]. We obtain a bond with predominant $(p_z p_z \sigma)$ character and an overlap population of 0.124 e, significantly lower than the usual Si-Si overlap population in the bulk of approximately 0.6 e. Such a bonding is also consistent with Northrup[19] who computed the total energy per adatom in a top site as to 0.64 eV lower than in a hollow site.

Our results can be eventually made compatible with a recent X-ray standing-wave (XSW) measurement by Durbin et al.[21] although it has been interpreted in another way, namely as a contraction in (111)-direction of the topmost two atom layers by 0.57 ± 0.16 A not counting the adatom layer as the topmost one since they purport the adatoms to be of no influence within their error bars. If the experiment is granted for being correct, at all, it can be reinterpreted along the following line of argument. We think that Durbin et al.[21] could have erroneously believed to have measured the distance between the surface and the third layer instead of the distance between the adatom layer and the second layer. They attribute an Auger electron yield proportional to $e^{-D_i/\lambda}$ to the i-th atom layer of the depth D_i where the mean free path λ of an Auger electron is assumed to be layer independent. Consisting of only 12 adatoms per 7x7 surface unit cell, a mean free path for the adatom layer about four times larger should be a better approximation resulting in an accordingly larger Auger electron yield, not too different from that of a bulk layer. Our computed adatom height over the second layer is 0.67 A shorter than the d_{111} lattice constant of 3.14 A appearing, thus, as the contraction of two planes by 0.57 ± 0.16 A as measured by Durbin *et al.*[21] (cf. Fig. 2b).

Tab. II shows the highest MOs of the electronic structure of our $Si_{28}H_{26}$ cluster. The surface atoms 2, 4, 8, 9 (cf. Fig. 2) give rise to four delocalized artificial surface states because they are not bonded to an adatom as in the real surface DAS-model. These delocalized artificial surface states MO 67-70 are easily identified by their AO composition in Tab. II, displaying all contributions ≥ 1 % to the MOs. MO 72 is the adatom surface state, first observed by Binnig *et al.*[22] with Scanning Tunneling Microscopy (STM). MO 71 has a 71 % AO contribution from the surface site (atom 6) and corresponds to one of the six (real) surface states of the 7x7 unit cell first identified by Hamers *et al.*[23] by using the same technique. According to our calculation, the adatom surface state consists of 39 % adatom contributions and 45 % AO contributions from the four next neighbours (atoms 3, 5, 7, 14; cf. Fig. 2) of the adatom and is, hence, delocalized over an Si_5 cluster with a geometry close to that of a trigonal bipyramid calculated in chapter 2.

A further means for testing the suitablity of the $Si_{28}H_{26}$ cluster modelling the Si(111)-7x7 surface is supplied by the comparison of our calculated ionization potentials (IPs) with other experimental[23] and theoretical[17] values. The IPs are given relative to the Fermi-Energy E_F, defined as the energy of the highest occupied state. The surface states at the adatom (MO 72), and at the surface site (MO 71) as well as the backbond (MOs 65 and 66) are most suitable for this comparison. Since the backbond MOs are nearly degenerate we define their IP as

$$IP(\text{backbond}) = \frac{IP(MO\ 66) + IP(MO\ 65)}{2} \pm \frac{IP(MO\ 66) - IP(MO\ 65)}{2}$$

The values for the respective MOs obtained in this way are given in Tab. III. The IPs calculated with the SCC-Xα Method match the experimental data slightly better than those of Qian and Chadi[17]. However, with respect to the size of the investigated systems, the maximum deviation of 0.2 eV has to be regarded as a good mutual agreement between both modes of calculation.

Considering the density of states (DOS) permits the qualitative comparison with photoelectron spectra (PES) when the discrete levels ϵ_k are folded by a Gaussian according to[16]

$$N(\epsilon) = \sum_k \frac{n_k}{\sqrt{2\pi}\,\sigma}\, e^{-\frac{1}{2}\left(\frac{\epsilon-\epsilon_k}{\sigma}\right)^2} \tag{4}$$

The DOS for the cluster $Si_{28}H_{26}$ is shown in Fig. 3a. The peak at E_F is attributed to the adatom surface state and the peak at about -6.3 eV arrises from the surface site. The next peak at -7.5 eV is constituted of dangling bonds of the surface atoms 2, 4, 8, 9 and is, therefore, a cluster artefact. The real surface states agree with the UV-PES from Demuth *et al.*[24] whereas more than qualitative agreement in the bulk region cannot be expected because, firstly, a cluster of only 28 Si atoms is not sufficient and secondly, Eq. (4) does not incorporate cross sections.

To assess the influence of the artificial dangling bonds of the surface atoms 2, 4, 8, 9 on the results so far obtained, the position of the surface site atom was varied again in a $Si_{28}H_{30}$ cluster where these bonds were saturated by one H-atom, respectively. In this case, the surface site atom moves closer to the surface by 0.002 A thus being negligible, and the IPs of the adatom and the backbond are E_f - 0.79 eV and E_f - (1.89 $\pm$ 0.04) eV, respectively. In spite of these minor improvements regarding the experimental data from Hamers *et al.*[23], the subsequent calculations on Ge adsorption on this substrate are performed with the unsaturated $Si_{28}H_{26}$ cluster because the changes seem to be too small to justify the additional computational effort for the larger cluster.

4. Ge-Adsorption on a Si(111)-7 x 7 Surface

The last set of calculations comprises the adsorption of a single Ge atom on the surface-atop site (atom 6 in Fig.2a), on the adatom-atop site (atom 1 in Fig.2a), and the coadsorption of two Ge atoms on both sites in the DAS-model. These investigations are intended to contribute to the understanding of the initial growth steps of thin Ge layers on silicon.

Dev et al.[25,26] have grown Ge on a Si(111)-7x7 substrate. According to their XSW measurements the Ge atoms are exclusively adsorbed on surface-atop sites for low coverages (up to Θ = 0.2 ML; 1 ML ≡ 49 Ge atoms per 7x7 unit cell) whereas for $\Theta \approx$ 0.4 ML Ge is adsorbed on the Si adatoms as well. The possibility of Ge adsorption on Si adatoms has been questionable so far.

Sarting with the adsorption of a single Ge atom on the surface-atop site of the $Si_{28}H_{26}$-cluster, we are comparing the electronic structure, Table IV, with that of the free cluster. The artificial surface states (MOs 69 - 72 in Tab.IV) are destabilized by only about 0.1 eV compared to the free cluster (cf.Tab.II) due to AO contributions of up to 2% from Ge p-orbitals. The nearly degenerate highest occupied MOs (HOMOs) 74 and 75 are lone pairs of the adsorbed Ge (atom 55). The dangling bond of the surface site Si-atom is pushed into the bulk states due to Ge adsorption as can be verified by comparing the DOS curve (Fig.3b) with that of the free cluster (Fig.3a). The minima in the DOS of the free cluster at -15.3 eV and -16.6 eV are less pronounced when Ge is adsorbed.

The SCC-Xα valence total energy as a function of the Si-Ge distance has been determined next. The calculated bond length of 2.638 A exceeds the Ge bulk bond length of 2.45 A considerably, most likely for the following reason. There is a spurious 16% AO contribution of the Ge atom to MO 73 (cf. Tab.IV) consisting otherwise of AOs from the trigonal bipyramid structure at the adatom (atoms 1, 3, 5, 7, 14). We suspect this to be caused by numerical instabilities during matrix diagonalization which may occasionally occur when many eigenvalues are closely spaced. It is quite improbable that therd exists a physical reason for this Ge AO contribution because of the separation of 4.60A

between the adatom and the Ge adsorbate which is also confirmed by the negligible overlap population of 0.008 e. The effect of this 16% spurious contribution is an increased amount of electron density attributed to the Ge atom, yielding an effective negative charge of -0.02 e, whereas a slightly positive charge on Ge should be expected in a Si-Ge bond. This argument gets support from another set of calculations where the Ge adsorption on the surface-atop site is repeated with the "saturated" $Si_{28}H_{30}$-cluster allowing to check the influence of the artificial surface states, too. In fact, this spurious AO-contribution vanishes when the Si substrate is modified in this way. However, these calculations could not be made convergent for all geometries since three almost degenerate MO's interchange during the iteration for some Si-Ge distances.

The next series of calculations investigates whether a Ge atom (atom 55) can be adsorbed on the adatom-atop site (atom 1). A minimum in the SCC-Xα total valence energy as a function of the Si-Ge distance (cf. Tab.VII) indicates clearly a stable bond. The electronic structure of the substrate-adsorbate system is given in Tab.VI, and Fig.3c shows the density-of-states curve. As expected, the free cluster surface state at the adatom (MO 72 in Tab.II) is pushed into the bulk states upon Ge adsorption on the adatom. The calculated equilibrium distance between the adatom and the adsorbed Ge is 2.339 A (cf. Tab.VII) and thus 0.299 A shorter than the corresponding bond length for surface-atop site adsorption. The overlap population of 0.842 e (cf. Tab.VII) between the adsorbed Ge and the Si adatom is distinctly larger than for surface-atop adsorption with an overlap population of 0.641 e (cf. Tab.V). However, this difference can be attributed mainly to the different bond lengths and does not tell anything about the preferred adsorption site. To find the energetically favourable adsorption site, one has to compare the total energies. For a single adsorbed Ge atom we obtain the total energy to be 2.502 eV per atom or 57.69 kcal/mole lower for surface-atop adsorption than for the

adatom-atop one. This value seems reasonable with respect to the bulk cohesive energies for Si (176 kcal/mole) and Ge (159 kcal/mole) even though we assume the true energy difference to be smaller by a factor of roughly 1.5 because Xα-procedures tend to overestimate binding energies in open shell systems[27] as is the substrate-adsorbate system dealt with here. The difference in total energy can easily be understood by comparing the two DOS curves for single adsorption. In the case of surface-atop adsorption (cf. Fig.3b), a smaller average density of states is recognized in the region from E_F down to roughly E_F - 13 eV than for adatom-atop adsorption (cf. Fig.3c), whereas the opposite is found in the interval between E_F - 13 eV and E_F - 19 eV. Thus, surface-atop adsorption of a Ge atom diminishes the density of surface-like states in favour of a higher density of bulk-like states to a larger extent than adatom-atop adsorption, leading eventually to a lower valence total energy in the former case.

Next we turn to the coadsorption of Ge on the surface site and the adatom site. The electronic structure is given in Tab.VIII, the valence total energy as a function of Si-Ge separations is listed in Tab.IX, and Fig.3d shows the DOS-curve. The IP's of the artificial dangling bonds (MO's 71 - 74 in Tab.VIII) are nearly unchanged if compared with both cases of single adsorption as well as to the bare cluster so that noticeable effects on the computed equilibrium geometry are not expected. The next four MO's 75 - 78 are Ge lone pairs with the lower two mainly located at the surface-atop site adsorbed Ge (atom 55) whereas the upper ones belong to the adatom-atop Ge (atom 56). With 85% AO contribution from atom 55, MO 76 is identified as the surface-atop adsorbate level and, analogously, MO 77 with 82% Ge p-orbital contributions is a lone pair from the Ge atom adsorbed on the adatom. The situation is less clear with MO's 75 and 78 because MO 75 contains a 34% contribution from atom 56 although the corresponding Ge lone pair MO 77 has a 0.264 eV higher IP. Likewise, MO 78 exhibits a 40% p-orbital contribution of atom 55 adsorbed on the surface site with its "true" lone pair MO 76 lower by 0.290 eV. This is striking because for adsorption of a single Ge atom the lone pairs are nearly degenerate, i.e.,

for surface-atop adsorption the separation between the Ge lone pairs is 0.011 eV (MO 74,75 in Tab.IV) and for adatom-atop adsorption the splitting is only 0.002 eV (MO 74,75 in Tab.VI).

The various bonds between the substrate and the adsorbate can be analyzed by comparing the dominant contributions that constitute the bond (cf. Tab.X) with each other. Two points should be emphysized. First, the Ge-Si-adatom bond has a significantly larger π-character and, second, the bond populations for single adsorption and coadsorption, respectively, are almost identical in both cases.

The effective charge of the surface-atop Ge atom is more positive by 0.029 e than that of the adatom-atop one which explains the ordering of the Ge lone pair MO's. This charge difference can be understood in terms of the larger distance of the Ge atom on the Si adatom to the average surface (defined by the atoms 2,3,4,5,7,8,9, cf. sect.3) leading to a small charge drift in direction of the respective outermost atoms that reflects the experimental situation, too. The computed effective Ge charges and Si-Ge bond lengths are as follows:

	coadsorption		single ads.
adsorption on	Q_{eff}(Ge)	d(Si,Ge)	d(Si,Ge)
adatom-atop	0.015 e	2.312 A	2.339 A
surface-atop	0.044 e	2.515 A	2.638 A

Whereas the Si-adatom-Ge bond length remains almost unchanged for coadsorption, a considerable shortening by 0.123 A of the Si-Ge bond length is obtained in case of surface-atop adsorption. This confirms our earlier assumption that the unreasonably large distance of 2.638 A may be due to a numerical instability.

By investigating, finally, the additional adsorption of a third Ge atom, we could show that breaking up the adatom structure yields a stable structure according to the experimentally observed transformation of the Si(111)-7x7

super structure into a perfect 1x1 surface upon Ge adsorption[28,29]. Thereby, two Ge atoms are adsorbed on the Si atoms 3 and 5 (cf. Fig.2) in the same way as the remaining Ge atom is in the surface-atop site. The former Si-adatom binds in an analogous manner to atom 7, albeit at a shorter distance. The calculated bond lengths are 2.386 A for the Si-Ge bond and 1.912 A for the Si-Si bond, respectively; the latter appears too short as a consequence of charge fluctuations leading to an unduly polar bond. According to this result, we expect the adatom structure to begin to break up at a Ge coverage of approximately 0.4 ML, nearly equivalent to the saturation of all Si dangling bonds in the DAS-model. This is consistent with the XSW results for higher coverages[35].

In order to understand the formation of this stable adsorption conformation, we have calculated, in a first step, the adsorption of the third Ge on top of that Ge atom adsorbed on the Si-adatom. Such an arrangement, however, turned out to be impossible, i.e. it did not lead to a stable geometry. To examine this process in more detail, possible reaction paths for the approach of an additional Ge atom have to be figured out when all Si adsorption sites are already occupied. To this end, further calculations are currently in progress to obtain the electrostatic potential in the vicinity of the Ge deposited surface in order to determine such reaction paths.

5. Comparison with Experiment.

Since no theoretical investigations of the Ge adsorption on Si(111)-7x7 surfaces have been published so far, we correlate our results only to the available experimental data. Gossmann et al.[28,29] report that the Si(111)-7x7 superstructure transforms into a perfect 1x1 surface upon Ge deposition of $\theta \approx 1.3$ ML at $T = 570$ K but that it does not take place at room temperature. This reconstruction is in accordance with our calculations insofar as the adsorption of a third Ge atom leads to a stable structure only if the adatom structure is broken up. However, our calculations correspond to Ge coverages of about 0.5 ML, and we didnot follow the growth process in detail. Consequently, a Ge coverage of $\theta = 1.3$ ML is too high for an instructive comparison with our calculations.

Patel et al.[30] deposited approximately 0.8 ML Ge on a Si(111)-7x7 substrate at a rate of about 1 ML/s which exceeds that of Gossmann et al.[28] by a factor of 600. Accordingly, it cannot be excluded that they have measured growth processes perturbed by Ge-Ge collisions during the adsorption. This effect could be significant because Patel et al.[30] have kept the substrate at room temperature during epitaxy thereby impeding the Ge atoms from finding their ideal adsorption site through surface diffusion. Furthermore, their interpretation is not based on an adatom model and assumes the upper two silicon surface layers unrelaxed. Moreover, they did not work under UHV conditions and added an amorphous silicon cap of 100 A to protect the Ge layer. According to Gibson et al.[31] such a cap preserves the 7x7 superstructure but presumably removes the adatom layer. Yet, in (111)-direction Patel et al.[30] observed a phase value of 1.02 d_{111} (d_{111}= 3.14 A) of the Fourier component of the Ge distribution function, close to the value of 1.06 d_{111} for θ_{Ge}= 0.4 ML measured by Dev et al.[25,26]

In a second paper, Patel et al.[32] base the interpretation of their XSW measurements under UHV conditions on the DAS-model but the Ge coverage of $\theta \approx 1$ ML

still does not allow any conclusion about the preferred adsorption site because an occupation of all six surface sites in a 7x7 unit cell corresponds to about 0.12 ML only. In (111)-direction they measured a phase value of 1.04 d_{111} with a coherent fraction of 0.44 but they did not give any details about the Ge positions concerning coverage sites. Therefore, it does not contain any valuable information with regard to our calculations.

Dev et al.[26] performed XSW measurements on the Ge/Si(111)-7x7 interface under UHV conditions for Ge coverages of 0.2 ML, 0.4 ML and 0.5 ML at a substrate temperature of 530° C. They interpret the coverage of 0.2 ML in the frame of the DAS-model as the Ge occupation of all six surface-atop sites, whereas the coverages of 0.4 ML and 0.5 ML are interpreted by the occupation of all atop sites; the latter value allows a small incoherent fraction from random positions. Thereby, Dev et al.[25,26] introduce three assumptions in their interpretation. First, they assume the height of the adatom over the first Si layer to be 0.78 A based on the STM experiments of Binnig et al.[22]. Secondly, the Si-Ge bond length is given the same value of 2.40 A for both adsorption sites which is the arithmetic average of the Si and Ge bulk bond lengths. Finally, they choose the Si bilayer separation also to be 0.78 A corresponding to an unrelaxed geometrical configuration. These assumptions have to be revised according to our results: On the one hand, the calculated Si-Ge bond lengths are substantially different for both adsorption sites. On the other hand, the adatom position deviates considerably from the assumed 1.56 A over the second layer. Remarkably, both errors almost cancel each other since, according to our calculations, the average Si-Ge bond length with six Ge atoms adsorbed on surface-atop sites and twelve on adatom-atop ones, corresponding to a coverage of about 0.4 ML Ge, is 2.38 A and thus close to 2.40 A. For a Ge coverage of 0.2 ML which equals an occupation of only the surface-atop sites, Dev et al.[25] measure in (111)-direction the Ge distance from the (111) diffraction plane which is the middle of the Si bilayer in absence of relaxation. The resulting

Si-Ge distance is 2.34 ± 0.06 A, a value being most likely too short. For, Becker et al.[34] observed a contraction by 0.2 A with STM in the faulted subcell of the DAS-model that would lead to a Si-Ge bond length of 2.44 A significantly closer to our results. Independently of this reasoning, a mechanism producing the effect that the Si-Ge bond length appears too short in the XSW experiments of Dev et al.[25] could be a possible contraction of the surface-atop site upon adsorption. Additionally, according to the recent calculation by Qian and Chadi[33] more than just the upper two Si layers exhibit a relaxation which seems more plausible than a relaxation of only the topmost two layers as reported by Takayanagi et al.[2] In summing up, we can conclude from our results that the actual Si-Ge bond length for direct surface-atop adsorption should range between 2.40 A and 2.52 A. Finally, taking the observations from Dev et al.[25,26] for granted, the interpretation of the XSW measurements by Durbin et al.[21] on the bare Si(111)-7x7 surface would require the unrealistic Si-Ge distance of 2.90 A supporting our reasoning in sect.3.

For θ_{Ge} = 0.4 ML Dev et al.[25] interpret their experiment as a complete Ge occupation of surface-atop and adatom-atop sites, the latter being possible only after all surface sites are occupied. This agrees exactly with our calculations that adatom adsorption of Ge is possible but distinctly less favourable. Such an interpretation gets further support by their measurements for Ge coverages of 0.2 ML and 0.5 ML in (220)-direction where the higher coverage corresponds to an occupation of all 18 adsorption sites in a 7x7 unit cell (or 19 including the corner hole). In this case, the observed Ge position was 0.75 d_{220} (d_{220} = 1.92 A) instead of 0.72 d_{220} as expected by them. This deviation is slightly above the given error bar of 0.01 d_{220}, the reason being simply the erroneous assumption of the too short adatom height, which gains importance with higher coverages when more Ge atoms are adsorbed on adatoms than on surface site atoms.

6. Conclusions

In this contribution, we have presented the first theoretical results about Ge adsorption on a reconstructed Si(111)-7x7 surface by cluster model calculations. Ge adsorption on adatoms is found to be possible but energetically less favourable than direct surface-atop adsorption, in agreement with experimental data. Thus, adatom adsorption takes place only after all surface sites are occupied. Our calculated distances are consistent with the available experimental data leading, at the same time, to revised interpretations in some cases. For Ge coverages higher than about 0.4 ML no additional Ge adsorption is possible without substantial structural changes. Stable structures are obtained by the rearrangement of the adatom structure, equivalent to the experimentally observed transformation from a 7x7 superstructure into a 1x1 lattice. A first theoretical explanation of the initial steps of Ge/Si(111)-7x7 interface formation has been tried. In order to understand this process in more detail, the electrostatic potential of the substrate-adsorbate system is currently being computed from the charge density at the cluster surface and between the adsorbates.

Acknowledgement

We wish to thank B.N.Dev and G.Materlik for helpful discussion on the experimental background and for reading the manuscript.

References

[1] K. Takayanagi, Y. Tanishiro, S. Takahashi, and M. Takahashi, Surf. Sci. 164, 367 (1985).

[2] K. Takayanagi, Y. Tanishiro, S. Takahashi, and M. Takahashi, J. Vac. Sci. Technol. A 3, 1502 (1985).

[3] M. Grodzicki, J. Phys. B 13, 2683 (1980).

[4] O. Kühnholz, Diplom thesis, Hamburg 1987.

[5] M. Grodzicki and O. Kühnholz, J. Molec. Struct. 174, 65 (1988).

[6] O. Zakharieva-Pencheva, H. Böse, H. Förster, W. Frede, and M. Grodzicki, J. Molec. Struct. 122, 101 (1985).

[7] H. Förster, M. Grodzicki, and O. Zakharieva-Pencheva, J. Molec. Struct. 143, 267 (1986).

[8] M. Grodzicki, H. Förster, R. Piffer, and O. Zakharieva-Pencheva, Catalysis Today 3, 75 (1988).

[9] M. Hütsch, Diplom thesis, Hamburg 1987.

[10] M. Hütsch and M. Grodzicki In: E. R. Hilf, F. Kammer, K. Wien (eds.), Lecture Notes in Physics 269, 212, Springer 1987.

[11] K. Raghavachari, J. Chem. Phys. 84, 5672 (1986).

[12] G. Pacchioni and J. Koutecky, J. Chem. Phys. 84, 3301 (1986).

[13] T. P. Martin and H. Schaber, Z. Phys. B 35, 61 (1979).

[14] K. Raghavachari and V. Logovinsky, Phys. Rev. Lett. 55, 2853 (1985).

[15] B. Kunz In: J. R. Smith (ed.), Theory of Chemisorption. Springer. Berlin, Heidelberg, New York 1980.

[16] R. P. Messmer In: T. N. Rhodin, G. Ertl (eds.): The Nature of the Surface Chemical Bond. North Holland. Amsterdam, New York, Oxford 1979.

[17] G. X. Qian and D. J. Chadi, Phys. Rev. B 35, 1288 (1987).

[18] M. Grodzicki, V. Männing, A. X. Trautwein, and J. M. Friedt, J. Phys. B 20, 5595 (1987).

[19] J. E. Northrup, Phys. Rev. Lett. 57, 154 (1986).

[20] W. Daum, H. Ibach, and J. E. Müller, Phys. Rev. Lett. 59, 1593 (1987).

[21] S. M. Durbin, L. E. Berman, and B. W. Batterman, Phys. Rev. Lett. 56, 236 (1986).

[22] G. Binnig, H. Rohrer, Ch. Gerber, and E. Weibel, Phys. Rev. Lett. 50, 120 (1983).

[23] R. J. Hamers, R. M. Tromp, and J. E. Demuth, Phys. Rev. Lett. 56, 1972 (1986).

[24] J. E. Demuth, B. N. J. Persson, and A. J. Schell-Sorokin, Phys, Rev. Lett. 51, 2214 (1983).

[25] B. N. Dev, G. Materlik, F. Grey, R. L. Johnson, and M. Clausnitzer, Phys. Rev. Lett. 57, 3058 (1986).

[26] B. N. Dev, G. Materlik, R. L. Johnson, W. Kranz, and P. Funke, Surf. Sci. 178, 1 (1986).

[27] O. Gunnarsson and R. O. Jones, Phys. Rev. B 31, 7588 (1985).

[28] H.-J. Gossmann, L. C. Feldman, and W. M. Gibson, Phys. Rev. Lett. 53, 294 (1984).

[29] H.-J. Gossmann, L. C. Feldman, and W. M. Gibson, Surf. Sci. 155, 413 (1985).

[30] J. R. Patel, J. A. Golovchenko, J. C. Bean, and R. J. Morris, Phys. Rev. B 31, 6884 (1985).

[31] J. M. Gibson, H.-J. Gossmann, J. C. Bean, R. T. Tung, and L. C. Feldman, Phys. Rev. Lett. 56, 355 (1986).

[32] J. R. Patel, P. E. Freeland, J. A. Golovchenko, A. R. Kortan, D. J. Chadi, and G. X. Qian, Phys. Rev. Lett. 57, 3077 (1986).

[33] G. X. Qian and D. J. Chadi, J. Vac. Sci. Technol. B 4, 1079 (1986).

[34] R. S. Becker, J. A. Golovchenko, E. G. McRae, B. S. Swartzentruber, Phys. Rev. Lett. 55, 2028 (1985).

[35] B.N.Dev, G.Materlik, F.Grey, and R.L.Johnson, to be published

Table I

Ground state and bond length of small silicon clusters.

	Pacchioni, Koutecky[12]		Raghavachari[11]		present work	
Cluster(Symmetry)	State:	bond length [A]	State:	bond length [A]	State:	bond length [A]
Si_4 (D_{4h})	$^3A_{2g}$:	d = 2.47	$^3A_{2g}$:	d = 2.316	$^3A_{2g}$:	d = 2.198
Si_4 (T_d)	$^3T_2$	d = 2.71	$^1A_1$:	d = 2.458	$^1A_1$:	d = 2.342
Si_5 (D_{3h})	$^3A_2'$:	d = 2.63	$^1A_1$:	$d_{lat-lat}$ = 3.256 d_{lat-ax} = 2.338	$^1A_1'$:	$d_{lat-lat}$ = 2.991 d_{lat-ax} = 2.342
Si_5 (C_{4v})	$^1A_1$:	d = 2.62	$^1A_1$:	$d_{lat-lat}$ = 2.295 d_{lat-ax} = 2.502	$^1A_1$:	$d_{lat-lat}$ = 2.306 d_{lat-ax} = 2.491
Si_5 (T_d)	^5E	d = 2.50	no values published		$^1A_{1g}$:	d = 2.171

Table II

Electronic structure of $Si_{28}H_{26}$ (cf. Fig. 2).

MO	65	66	67	68	69	70	71	72
IP (eV)	7.405	7.333	6.507	6.465	6.349	6.324	6.285	5.465
	AO contributions to MO (in % of MO)							
1 Si 3s [a)]	0	0						8
1 Si 3p [a)]	7	10						31
2+9 Si 3s [b)]			8	7	5	6	0	
2+9 Si 3p [b)]			42	42	25	29	3	
4+8 Si 3s [b)]			4	5	9	9	0	
4+8 Si 3p [b)]			21	27	46	47	3	
3+7 Si 3s [c)]	2	0						3
3+7 Si 3p [c)]	51	17						26
5 Si 3s [d)]	0	2						2
5 Si 3p [d)]	1	35						12
6 Si 3s [e)]			2				8	
6 Si 3p [e)]			8				63	
14 Si 3s [f)]	0	0						1
14 Si 3p [f)]	28	28						1

a) Adatom.

b) Surface atom. Due to symmetry both atoms yield the same AO contributions. Therefore no information is lost by their addition.

c) Surface atom saturated by adatom. Due to symmetry both atoms yield the same AO contributions. Therefore no information is lost by their addition.

d) Surface atom saturated by adatom.

e) Surface site.

f) Second layer atom under adatom.

Table III

Comparison of selected surface states from various sources.

source	Hamers *et al.*[23]	Qian, Chadi[17]	present work
state	[Experiment]	[Theory]	[Theory]
adatom	E_F - 0.2 eV	E_F	E_F
surf. site	E_F - 0.8 eV	E_F - 0.9 eV	E_F - 0.82 eV
backbond	E_F - 1.7 eV	E_F - 1.5 eV	E_F - (1.90 ± 0.04) eV

Table IV

Electronic structure of $Si_{28}H_{26}$ for adsorption of a single Ge atom (atom 55) on the surface site (atom 6).

MO	69	70	71	72	73	74	75
IP (eV)	6.431	6.429	6.294	6.264	5.601	5.545	5.534
	AO contributions to MO (in % of MO)						
1 Si 3s [a]					6		2
1 Si 3p [a]					26		7
2+9 Si 3s [b]	9	8	4	4		0	
2+9 Si 3p [b]	49	49	21	23		2	
4+8 Si 3s [b]	3	3	9	10		0	0
4+8 Si 3p [b]	18	20	50	53		1	1
3+7 Si 3s [c]					3		0
3+7 Si 3p [c]					24		4
5 Si 3s [d]					1		1
5 Si 3p [d]					9		4
14 Si 3s [e]					1		
14 Si 3p [e]					1		
55 Ge 4s [f]	0	0	0		0	0	0
55 Ge 4p [f]	1	2	1		16	95	74

a) Adatom.

b) Surface atom. Due to symmetry both atoms yield the same AO contributions. Therefore no information is lost by their addition.

c) Surface atom saturated by adatom. Due to symmetry both atoms yield the same AO contributions. Therefore no information is lost by their addition.

d) Surface atom saturated by adatom.

e) Second layer atom under adatom.

f) Germanium adsorbate.

Table V

SCC-Xα valence total energy as a function of the Si-Ge bond length between the surface site (atom 6) and single Ge (atom 55) adsorbed thereon.

ΔE_{total} relative to the valence total energy minimum at d(6Si, 55Ge) = 2.638 Å

d(6Si, 55Ge) [a.u.]	d(6Si, 55Ge) [Å]	E_{total} [Ry]	ΔE_{total} [Kcal/mol]	overlap population of 55Ge with 6Si	13Si = 17Si	15Si
4.735	2.506	-139.904	5.011	0.712	-0.038	-0.039
4.835	2.559	-139.913	2.189	0.683	-0.036	-0.037
4.935	2.612	-139.920	0.051	0.656	-0.034	-0.034
4.986	2.638	-139.920	≡ 0	0.641	-0.032	-0.033
5.035	2.665	-139.919	0.433	0.631	-0.031	-0.032

Table VI

Electronic structure of $Si_{28}H_{26}$ for adsorption of a single Ge atom (atom 55) on the adatom (atom 1).

MO	69	70	71	72	73	74	75
IP (eV)	6.478	6.435	6.320	6.296	6.250	5.635	5.633
	AO contributions to MO (in % of MO)						
2+9 Si 3s [a]	8	7	5	6	0		
2+9 Si 3p [a]	43	44	25	29	4		
4+8 Si 3s [a]	4	5	9	9	0		
4+8 Si 3p [a]	21	27	47	47	2		
3+7 Si 3s [b]						2	0
3+7 Si 3p [b]						8	3
5 Si 3s [c]							1
5 Si 3p [c]							5
6 Si 3s [d]	1				8		
6 Si 3p [d]	8				63		
55 Ge 4s [e]						0	0
55 Ge 4p [e]						89	88

a) Surface atom. Due to symmetry both atoms yield the same AO contributions. Therefore no information is lost by their addition.
b) Surface atom saturated by adatom. Due to symmetry both atoms yield the same AO contributions. Therefore no information is lost by their addition.
c) Surface atom saturated by adatom.
d) Surface site.
e) Germanium adsorbate.

Table VII

SCC-Xα valence total energy and overlap population as a function of the Si-Ge bond length between the adatom (atom 1) and single Ge (atom 55) adsorbed thereon.

Variation the bond length d(1Si, 55Ge)

ΔE_{total} relative to the valence total energy minimum at d(1Si, 55Ge) = 2.339 A

d(1Si, 55Ge) [a.u.]	[A]	E_{total} [Ry]	ΔE_{total} [Kcal/mol]	overlap population of 55Ge with 1Si	3Si = 7Si	5Si
4.235	2.241	-139.697	11.95	0.926	-0.038	-0.034
4.335	2.294	-139.731	1.383	0.881	-0.038	-0.034
4.421	2.339	-139.736	≡ 0	0.842	-0.038	-0.034
4.435	2.347	-139.735	0.034	0.834	-0.038	-0.034
4.535	2.400	-139.730	1.790	0.792	-0.037	-0.033
4.735	2.506	-139.709	8.250	0.712	-0.034	-0.031

Table VIII

Electronic structure of $Si_{28}H_{26}$ for coadsorption of two Ge atoms.
Atom 55Ge is adsorbed on the surface site (atom 6)
and atom 56Ge is adsorbed on the adatom (atom 1).

MO	71	72	73	74	75	76	77	78
IP (eV)	6.463	6.459	6.335	6.305	5.889	5.713	5.625	5.423
	AO contributions to MO (in % of MO)							
2+9 Si 3s [a]	6	6	7	5		0		
2+9 Si 3p [a]	39	37	33	31		1		
4+8 Si 3s [a]	5	5	7	8	0	0		
4+8 Si 3p [a]	29	29	39	45	2	1		
3+7 Si 3s [b]					0	0	2	0
3+7 Si 3p [b]					3	1	7	1
5 Si 3s [c]					1			0
5 Si 3p [c]					3			3
55 Ge 4s [d]	0	0	0		0	0	0	0
55 Ge 4p [d]	4	2	1		53	85	7	40
56 Ge 4s [e]					0	0	0	0
56 Ge 4p [e]					34	6	82	53

a) Surface atom. Due to symmetry both atoms yield the same AO contributions. Therefore no information is lost by their addition.
b) Surface atom saturated by adatom. Due to symmetry both atoms yield the same AO contributions. Therefore no information is lost by their addition.
c) Surface atom saturated by adatom.
d) Germanium adsorbate on the surface site.
e) Germanium adsorbate on the adatom.

Table IX

SCC-Xα valence total energy and overlap population for coadsorption as a function of the Si-Ge bond length between the surface site (atom 6) and a Ge (atom 55) adsorbed thereon as well as the adatom (atom 1) and a Ge (atom 56) adsorbed thereon.

Variation of the bond length d(1Si, 56Ge)

ΔE_{total} relative to the valence total energy minimum at d(1Si, 56Ge) = 2.312 A

d(1Si, 56Ge) [a.u.]	[A]	E_{total} [Ry]	ΔE_{total} [Kcal/mol]	overlap population of 56Ge with 1Si	3Si = 7Si	5Si
4.285	2.268	-143.133	6.290	0.906	-0.038	-0.035
4.335	2.294	-143.152	0.364	0.883	-0.038	-0.035
4.370	2.312	-143.153	≈ 0	0.868	-0.037	-0.035
4.385	2.321	-143.153	0.051	0.861	-0.037	-0.035
4.435	2.347	-143.150	0.709	0.838	-0.037	-0.034
4.485	2.376	-143.148	1.399	0.816	-0.037	-0.034
4.535	2.400	-143.147	1.775	0.795	-0.036	-0.034

Variation of the bond length d(6Si, 55Ge)

ΔE_{total} relative to the valence total energy minimum at d(6Si, 55Ge) = 2.515 A

d(6Si, 55Ge) [a.u.]	[A]	E_{total} [Ry]	ΔE_{total} [Kcal/mol]	overlap population of 55Ge with 6Si	13Si = 17Si	15Si
4.585	2.426	-143.142	6.368	0.756	-0.042	-0.041
4.635	2.453	-143.150	3.640	0.741	-0.041	-0.040
4.735	2.506	-143.162	0.097	0.711	-0.039	-0.038
4.754	2.515	-143.162	≈ 0	0.707	-0.038	-0.038
4.835	2.559	-143.153	2.919	0.683	-0.037	-0.036
4.935	2.612	-143.133	9.190	0.656	-0.035	-0.034

Table X

Dominant contributions to the overlap population of the various Si-Ge adsorption bonds.

bond	adatom adsorption: single	adatom adsorption: coadsorption	surface site adsorption: single	surface site adsorption: coadsorption
(Si 3p, Ge 4p, σ)	0.37	0.37	0.47	0.47
(Si 3s, Ge 4p, σ)	0.25	0.25	0.16	0.18
(Si 3p, Ge 4s, σ)	0.12	0.12	0.03	0.06
(Si 3p, Ge 4p, π)	0.13	0.14	0.01	0.02

Figure Captions.

Fig. 1: Si_5-cluster in (a) D_{3h}-symmetry (trigonal bipyramid) with the lateral atoms 1,2,3 and the axial atoms 4,5; (b) C_{4v}-symmetry with the axial atom 1 and the lateral atoms 2,3,4,5; (c) T_d-symmetry with the central atom 1 and the peripheral atoms 2,3,4,5.

Fig. 2a: Top view of the Si atoms of the free $Si_{28}H_{26}$-cluster with the adatom 1 and the surface site 6. The second layer atom 14 under the adatom is hidden from view.

Fig. 2b: Side view of the adatom layer and the first four layers of the unrelaxed Si(111)-surface within a plane determined by atoms 1,5,6 and 14. The diffraction plane d_{111} is the middle of the Si-bilayer and d_{bi} is the bilayer separation. The computed distance d_{a2} between the second and the adatom layer is by 0.67 A shorter than d_{111}. There is no direct bonding between the adatom 1 and the surface site atom 6. The atoms 3 and 7 directly bonded to the adatom are above and below the plane (indicated by dotted circles).

Fig. 3a: Density-of-states (DOS) curve for the free $Si_{28}H_{26}$-cluster. Here and in the subsequent DOS-plots, E_F is defined as the energy of the highest occupied state.

Fig. 3b: DOS-curve for the $Si_{28}H_{26}$-cluster with one Ge atom adsorbed on the surface site (atom 6 in Fig.2)

Fig. 3c: DOS-curve for the $Si_{28}H_{26}$-cluster with one Ge atom adsorbed on the adatom site (atom 1 in Fig.2)

Fig. 3d: DOS-curve of the $Ge_2Si_{28}H_{26}$-cluster for coadsorption on the adatom and on the surface site atom.

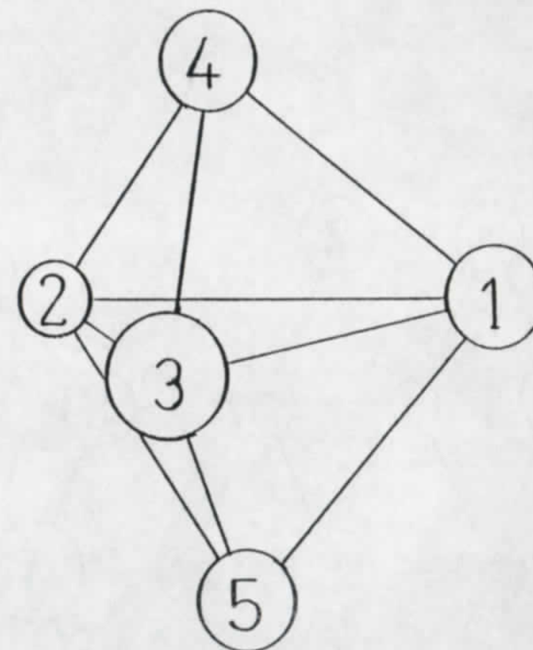

Fig. 1(a)

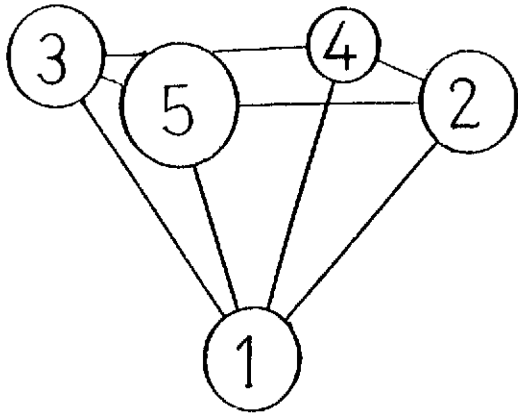

Fig. 1(b)

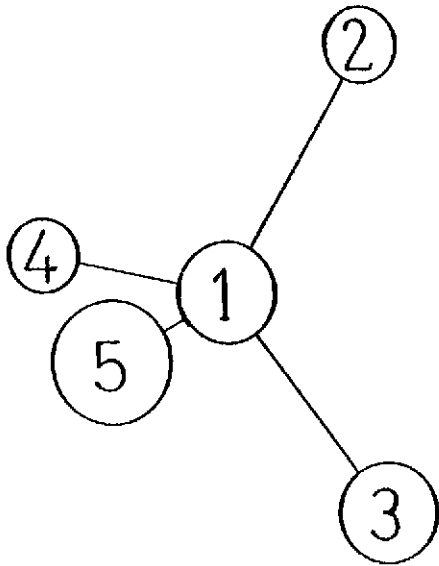

Fig. 1(c)

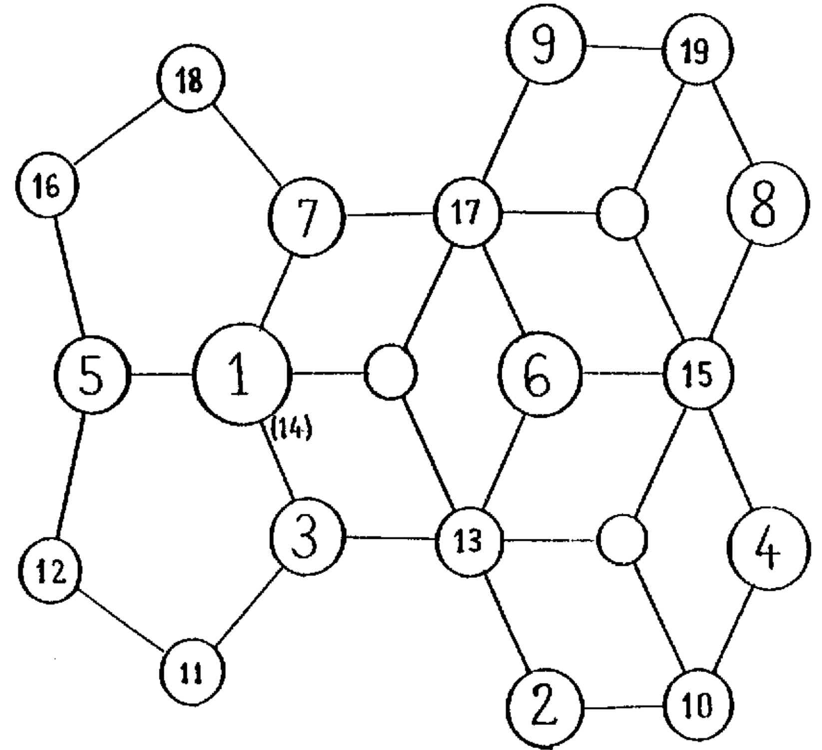

Fig. 2(a)

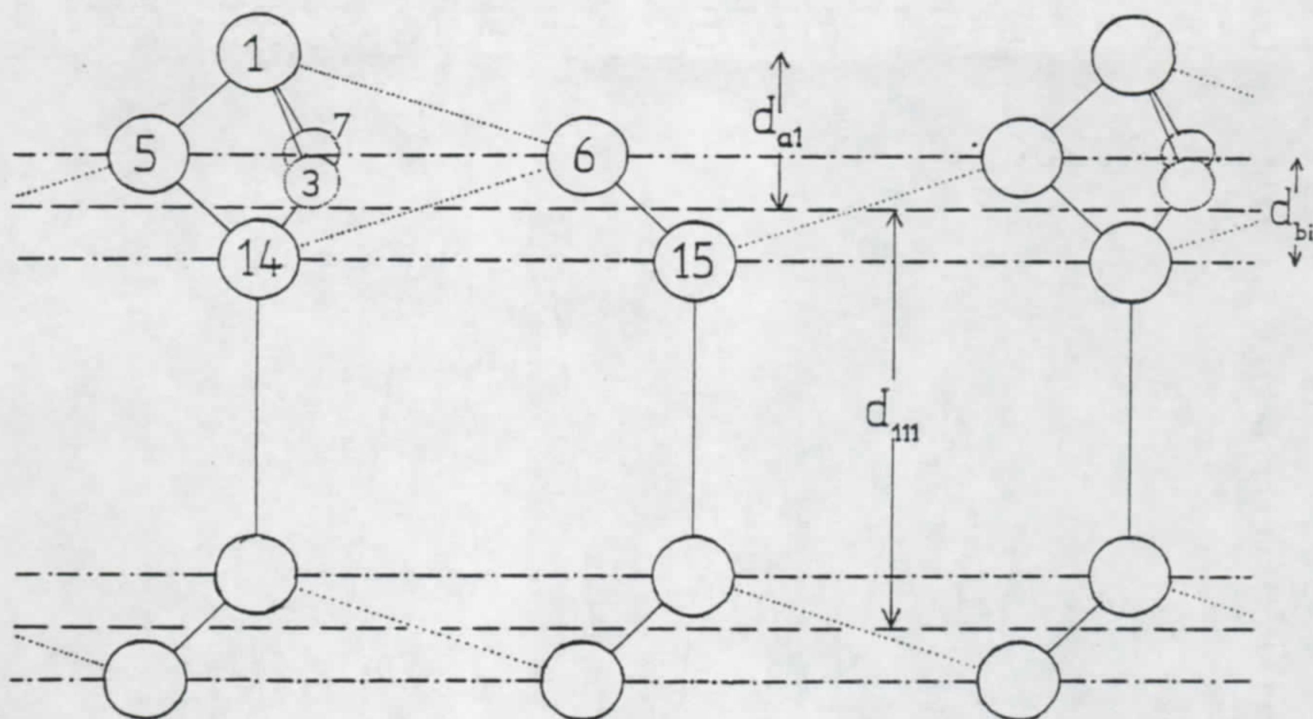

Fig. 2(b)

DOS for __SI28H26_____NO_GE__

σ= 0.200 eV

Density of States (Arb.U.)

0 5 10 15

-20 -18 -16 -14 -12 -10 -8 -6 -4

E_F

Energy (eV)

Fig. 3(a)

DOS for __SI28H26__GE_ON_SURFACE__

σ= 0.200 eV

Density of States (Arb.U.)

0 5 10 15

-20 -18 -16 -14 -12 -10 -8 -6 -4

E_F

Energy (eV)

Fig. 3(b)

DOS for __SI28H26__GE_ON_ADATOM__

σ= 0.200 eV

Density of States (Arb.U.)

0 5 10 15

-20 -18 -16 -14 -12 -10 -8 -6 -4

E_F

Energy (eV)

Fig. 3(c)

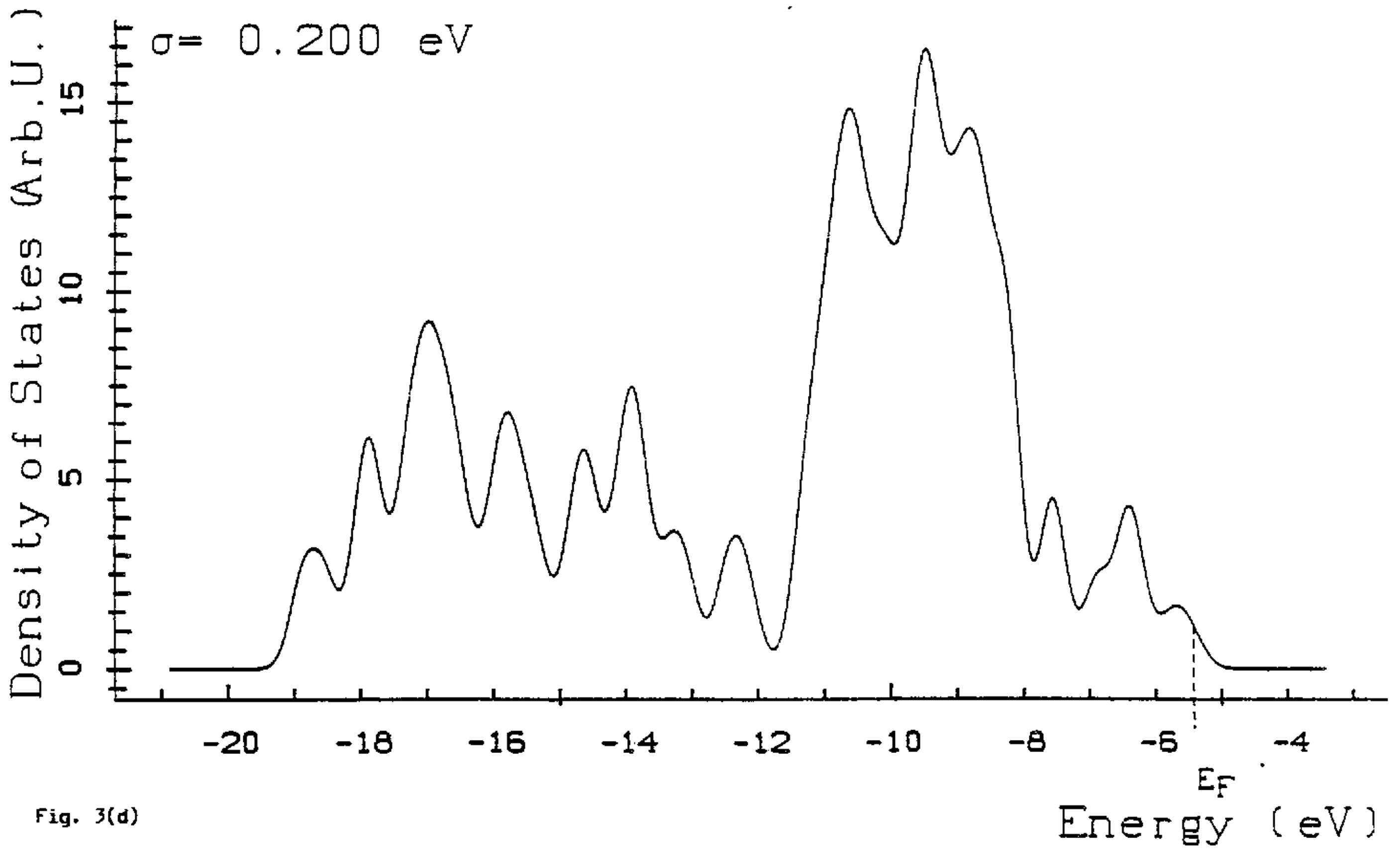

Fig. 3(d)